The Vertical Profile of Liquid and Ice Water Content in Midlatitude Mixed-Phase Altocumulus Clouds

LAWRENCE D. CAREY, JIANGUO NIU, AND PING YANG

Department of Atmospheric Sciences, Texas A&M University, College Station, Texas

J. ADAM KANKIEWICZ

U.S. Department of Defense Center for Geosciences/Atmospheric Research, Colorado State University, Fort Collins, Colorado

VINCENT E. LARSON

Department of Mathematical Sciences, University of Wisconsin—Milwaukee, Milwaukee, Wisconsin

THOMAS H. VONDER HAAR

U.S. Department of Defense Center for Geosciences/Atmospheric Research, Colorado State University, Fort Collins, Colorado, and Department of Atmospheric Sciences, Texas A&M University, College Station, Texas

(Manuscript received 1 October 2007, in final form 4 February 2008)

ABSTRACT

The microphysical properties of mixed-phase altocumulus clouds are investigated using in situ airborne measurements acquired during the ninth Cloud Layer Experiment (CLEX-9) over a midlatitude location. Approximately ⅔ of the sampled profiles are supercooled liquid–topped altocumulus clouds characterized by mixed-phase conditions. The coexistence of measurable liquid water droplets and ice crystals begins at or within tens of meters of cloud top and extends down to cloud base. Ice virga is found below cloud base. Peak liquid water contents occur at or near cloud top while peak ice water contents occur in the lower half of the cloud or in virga. The estimation of ice water content from particle size data requires that an assumption be made regarding the particle mass–dimensional relation, resulting in potential error on the order of tens of percent. The highest proportion of liquid is typically found in the coldest (top) part of the cloud profile. This feature of the microphysical structure for the midlatitude mixed-phase altocumulus clouds is similar to that reported for mixed-phase clouds over the Arctic region. The results obtained for limited cases of midlatitude mixed-phase clouds observed during CLEX-9 may have an implication for the study of mixed-phase cloud microphysics, satellite remote sensing applications, and the parameterization of mixed-phase cloud radiative properties in climate models.

1. Introduction

At temperatures between 0° and −40°C, liquid water droplets and ice crystals may coexist in a single-layered cloud. Although studies have indicated that the parameterization of so-called mixed-phase clouds is critical for understanding the radiative characteristics of clouds in climate models and satellite remote sensing applications (e.g., Li and Le Treut 1992; Sun and Shine 1995; Gregory and Morris 1996; Hogan et al. 2002; Yang et al. 2003; McFarquhar and Cober 2004), relatively little is known about their microphysical properties.

The vertical distribution of liquid water content (LWC) and ice water content (IWC) is of primary importance for modeling radiative transfer within clouds under mixed-phase conditions (Niu et al. 2008). Recent

Corresponding author address: Dr. Ping Yang, Department of Atmospheric Sciences, Texas A&M University, College Station, TX 77843.
E-mail: pyang@ariel.met.tamu.edu

DOI: 10.1175/2008JAMC1885.1

in situ measurements (e.g., Fleishauer et al. 2002; Korolev et al. 2003) demonstrate that the distributions of liquid and ice water content versus temperature in mixed-phase clouds are complex. Nonetheless, previous observations suggest a common feature for the vertical profiles of liquid and ice water for single-layer mixed-phase clouds. To be specific, observations of both boundary layer mixed-phase clouds (e.g., Pinto 1998; Lawson et al. 2001; Zuidema et al. 2005; Verlinde et al. 2007; McFarquhar et al. 2007) and midlevel mixed-phase clouds (e.g., Hobbs and Rangno 1998; Pinto et al. 2001; Hobbs et al. 2001) over the Arctic region indicate that the dominant presence of liquid (ice) water in the upper (lower) portions of these clouds is likely a common feature. For example, Hobbs et al. (2001) presented in situ observations of a single-layered Arctic altocumulus cloud consisting of a thin, slightly supercooled liquid water cloud with ice virga below. Numerical simulations (e.g., Harrington et al. 1999) also reproduced a similar microphysical structure for Arctic boundary layer stratus clouds.

However, in the midlatitude region, fewer observations of mixed-phase clouds have been reported. Rauber and Grant (1986) investigated winter storm clouds over mountainous areas. They observed a supercooled water layer existing at the cloud top and concluded that the supercooled water can be produced in any region where the condensation rate exceeds the diffusional growth rate of ice crystals. Hobbs and Rangno (1985) observed two different types of altocumulus clouds (castellanus and floccus) by a simple flight track through cloud top and bottom. In their study, a liquid water content maximum coexisted with a small number of ice particles at cloud top while a large concentration of ice particles was found at cloud bottom without liquid water content. Heymsfield et al. (1991) investigated two cases of altocumulus clouds. In one case, they found a thin, highly supercooled liquid water layer located at the top of the altocumulus cloud. Fleishauer et al. (2002) observed an increase of liquid water content with altitude in single-layer clouds, whereas the ice water content maximized in the middle to lower parts of the cloud. Using ground-based radar and lidar and in situ aircraft, Hogan et al. (2002) presented observations of a single altocumulus cloud consisting of a supercooled water layer with ice particle fall streaks below. Wang et al. (2004) recently demonstrated a combined active and passive remote sensing approach for studying supercooled altocumulus with ice virga. These limited observations prompt a simple question: Is supercooled liquid and mixed-phase cloud above ice virga a common feature for midlevel mixed-phase altocumulus (AC) clouds in the midlatitude region as has been found for Arctic clouds?

2. Observations and method

The Cloud Layer Experiment (CLEX), aimed at a better understanding of mixed-phase clouds in the middle troposphere, was started in 1996 (Larson et al. 2001; Fleishauer et al. 2002). CLEX-9 was conducted over western Nebraska from 8 October through 4 November 2001 with the deployment of the University of Wyoming King Air research aircraft (UWKA). The particle measurement systems mounted on this aircraft allow in situ observations of cloud microphysical parameters. The CLEX-9 microphysical observations presented herein are the first overview analysis in the peer-reviewed literature of this important and unique dataset of midlatitude mixed-phase altocumulus clouds.

The Particle Measuring Systems (PMS) two-dimensional cloud and precipitation (2DC and 2DP, respectively) probes provided measurements of the ice particle size distribution (PSD). The PMS 2DC and 2DP collect particles with maximum diameters that range from 25 to 6500 μm and from 100 to 9000 μm, respectively. A PMS Forward Scattering Spectrometer Probe (FSSP) measured the PSD of water droplets, with 16 bins covering particle sizes from 1 to 31 μm with a 2-μm bin interval. The PMS FSSP, Rosemount 871FA icing detector, Gerber PVM-100A, and Droplet Measurement Technology (DMT) model LWC-100 provided simultaneous observations of liquid water content. The Rosemount icing detector has been used to detect the presence of supercooled water in mixed-phase clouds. Its linear response to the LWC when temperatures are lower than -4°C without sensitivity to ice particles makes the instrument an ideal choice for detecting the presence of supercooled water (Cober et al. 2001c). Rosemount probe data in this work have been used to provide a threshold for removing the noise and ice contamination in the FSSP data. Detailed discussion of the analysis technique, limitations, and accuracy for each of the key cloud probes used in this study can be found in Heymsfield and Parrish (1978), Baumgardner (1983), and Cerni (1983). Specific processing techniques used to increase the confidence of the determined particle phase, size distribution, and water content are discussed in detail below. Thermodynamic parameters (e.g., temperature) were measured by various instruments such as the Reverse Flow and Rosemount thermometers.

To obtain cloud microphysical properties in the vertical direction, different types of aircraft flight tracks were used. The simplest route was a direct ascending or

descending track, which is a slant leg from cloud bottom to top or vice versa. A ladderlike route included repeated slant-up (-down) and horizontal-level tracks. In the descending (ascending) Lagrangian spiral, the aircraft flew down (up) spirally from cloud top to base (or vice versa) while drifting with the horizontal environmental winds. Last, in the so-called porpoise route, the aircraft repeated direct ascending and descending tracks in a gentle (i.e., wavelength = 25–30 km) sinusoidal pattern between cloud top and bottom. The porpoise route was effective for sampling the vertical structure of thin (i.e., 100–300 m) clouds.

The IWC was estimated from a combination of the PMS 2DC and 2DP measured ice PSDs. The PMS 2DC and 2DP PSD data were first processed to remove noise and various artifacts according to procedures at the University of Wyoming, including a simple shape-based test to remove water contamination from the 2DC/2DP ice PSD data.[1] Because our target clouds were nonprecipitating, the typical size spectrum of ice particles (i.e., typical mode of several hundred micrometers) was well sampled by the 2DC probe. However, the 2DP probe was often more sensitive to the presence of the largest ice particles than was the 2DC (i.e., the 2DP often measured significantly more large particles in the tail of the size distribution). In those situations, the ice particle concentrations from the two probes crossed over each other at a critical diameter typically between 2 and 3 mm. In the estimation of IWC, the 2DC (2DP) PSD was used for diameters that were less (greater) than the critical diameter, providing a smooth and continuous curve of ice concentration that is more accurate than using the 2DC or 2DP alone. The critical diameter was determined separately for each vertical cloud profile. By following the method of Fleishauer et al. (2002), the average IWC was then calculated every 10 s (or roughly every 50 m in the vertical direction) from the combined PMS 2DC/2DP PSD by using the all-snow mass–dimensional relationship reported by Mitchell et al. (1990). To test the sensitivity of our IWC estimates to the averaging period, a variety of times from 10 to 30 s (from 50 to 150 m in the vertical direction) were employed. As expected, the longer averaging period of 30 s created a smoother curve with maxima (minima) that were as much as 15% lower (higher) in magnitude. The vertical profiles of IWC from all of the averaging periods were highly correlated, placing maxima and minima in similar locations in the vertical direction. Because our mixed-phase clouds are relatively shallow, we chose the shorter averaging period so as to retain vertical structure in the clouds. The assumption of the mass–dimensional relation can introduce significant variability (or error) in the estimation of the IWC from PSD data. To bracket this variability, we compared our results with other well-known relations. The commonly used Brown and Francis (1995) mass–dimensional relation resulted in a 49% positive bias relative to our IWC results with Mitchell et al. (1990). On the other hand, the more advanced technique for extracting IWC from PSD data of Heymsfield et al. (2002), which uses a two-parameter approach that includes the projected cross-sectional area in addition to the maximum projected diameter, resulted in a 23% negative bias relative to our results. Despite the difference in the IWC estimates, the IWC profiles from each of the three methods were highly correlated such that maxima and minima were generally collocated. Hence, the key results herein were not sensitive to assumptions regarding the ice mass–dimensional relation.

The LWC used in this study was estimated from the FSSP-100 particle size distribution. The FSSP-estimated LWC was identified as noise or ice contamination and then was deleted when the estimated Rosemount LWC was less than a threshold value of 0.002 g m^{-3}. This Rosemount LWC threshold was selected based on the assessments of the Rosemount icing detector conducted by Cober et al. (2001a, b). The reasons for using FSSP-100 estimated LWC are threefold. First, as already mentioned, the FSSP-100 can provide measurements of the droplet particle size distribution, which are required for our ongoing studies of the radiative properties of these clouds (Niu et al. 2008). Second, the in-cloud stability of the LWC derived from the FSSP-100 is the same as that of the Gerber PVM-100A probe and is better than that of the Rosemount icing and DMT-100 probes. Third, the FSSP provides cloud profiles of LWC that are similar to those of the Gerber and other probes (when they are stable) for all cases. In this study, we have quantitatively compared FSSP and Gerber LWCs in a typical mixed-phase case (see Fig. 1h for FSSP LWC only). Following the method of Fleishauer et al. (2002), we removed the bias in the Gerber LWC by subtracting an obvious linear offset with height (i.e., air density). Although absolute differences in LWC between the two probes can be large (up to 0.04 g m^{-3}) at times, the mean and maximum relative differences between the FSSP and Gerber LWCs were only 12% and 28%, respectively. In a similar way, Niu et al. (2008) compared the Rosemount- and FSSP-derived LWCs for a selected mixed-phase profile (see Fig. 1d for FSSP LWC only) and found them to be

[1] Further information about the UWKA processing of probe data can be found online at http://flights.uwyo.edu/ka_doc/index.html.

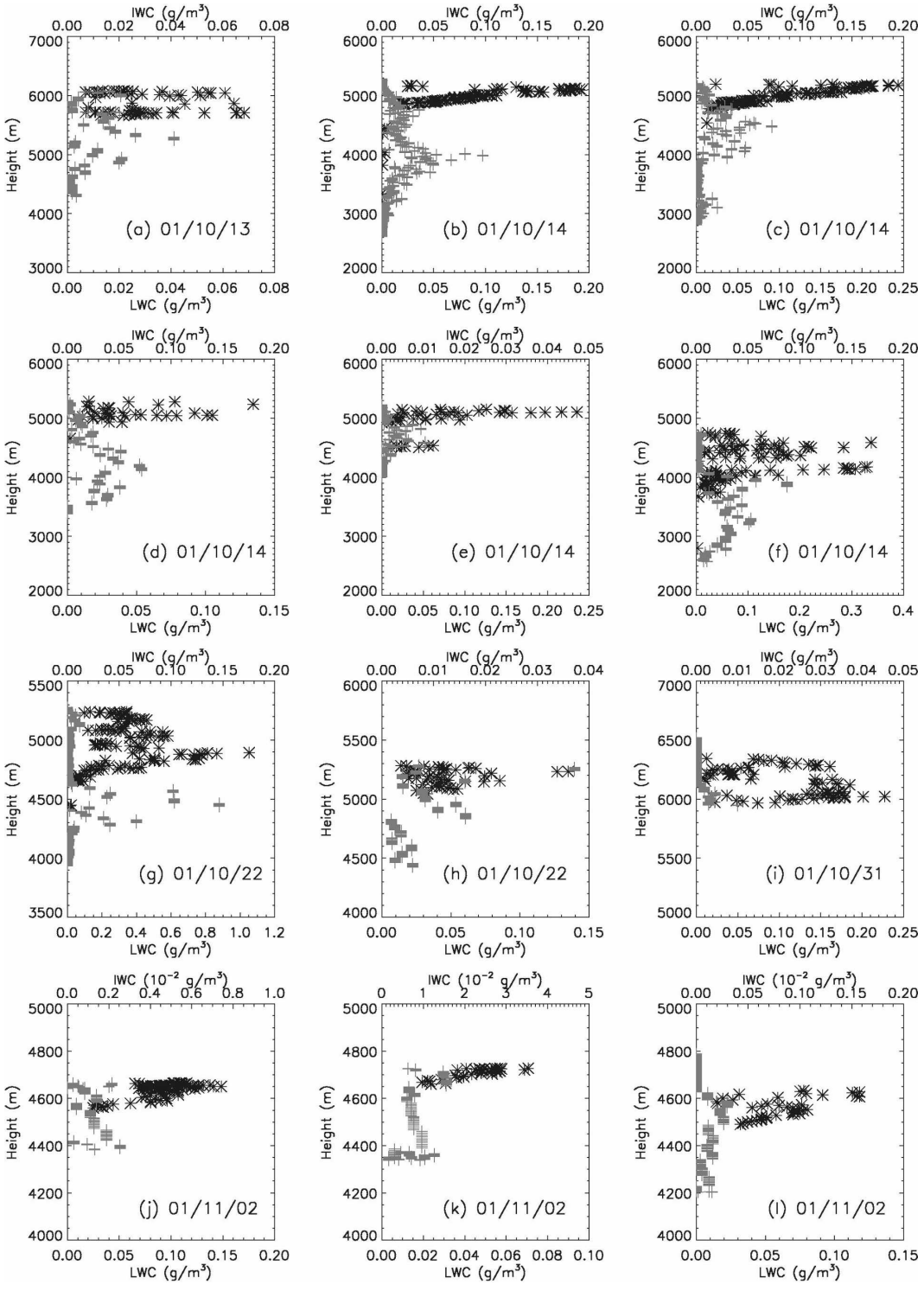

FIG. 1. Typical vertical profiles of LWC (g m^{-3}; black asterisks) and IWC (g m^{-3}; gray pluses) within midlevel mixed-phase clouds over the midlatitude region as measured during the CLEX-9 field campaign. The date of each observation is indicated by YY/MM/DD, where DD is day, MM is month, and YY is last two digits of year: 20YY. Note the different scales for LWC (*x* axis below panel) and IWC (*x* axis above panel) for each profile.

highly correlated. The FSSP LWC was slightly positively biased relative to the Rosemount LWC, with a maximum bias of 5% at the larger LWCs. Despite known limitations of the FSSP and 2DC/2DP for estimating LWC and IWC, respectively, in mixed-phase clouds (e.g., Fleishauer et al. 2002), we are confident that the qualitative vertical structure of water content is independent of potential biases and errors.

3. Results

During CLEX-9, the UWKA completed 10 separate flight missions during eight different days (12, 13, 14, 19, 22, and 31 October and 1–2 November 2001). More than 16 h of in-cloud observational data were obtained during these flight missions. After elimination of horizontal flights legs and incomplete vertical cloud penetrations from the in-cloud observational dataset, a total of 30 vertical cloud profiles were obtained from different types of descending and ascending observational legs. Twenty out of the 30 vertical cloud profiles from five different observation days are clearly recognized as water-dominated mixed-phase altocumulus clouds with ice virga below, which are partly illustrated in Fig. 1 in chronological order from Fig. 1a to Fig. 1l. The remaining 10 other clouds (not shown) are ice particle–dominated or glaciated clouds with little or no supercooled LWC (i.e., maximum LWC < 0.02 g m^{-3}).

The temperature (height) of the supercooled liquid cloud top varies from $-13°$ to $-26°$C (from 4600 to 6300 m). The temperature variation is typically 1°–3°C between the bottom and top of the supercooled liquid layer. However, for thicker water clouds such as seen in Figs. 1f and 1g, the temperature variation can be much larger (i.e., 4°–6°C). The average thickness of the upper supercooled liquid cloud layer is about 350 m and can be as small as 80 m or as large as 1000 m. The altitude of the maximum LWC varies from 4600 to 6000 m and is typically at or near cloud top. In fact, the altitude of the peak LWC is within the upper half of the cloud water layer in 9 of 12 AC profiles, similar to the results of Fleishauer et al. (2002). A notable exception can be found in Fig. 1i, in which the altitude of the peak LWC occurs within 70 m of cloud base.

Inspection of the Wyoming Cloud Radar (WCR) radar reflectivity structure in the vertical direction (not shown) during the direct descending cloud profile in Fig. 1i suggests that horizontal variability may have caused this departure from typical behavior. To be more specific, horizontal variability in the cloud-top height of the AC field revealed in the WCR reflectivity data may have resulted in the maximum LWC being placed near the bottom of the profile in Fig. 1i. In reality, the peak LWC within 70 m of what appears to be "cloud base" in Fig. 1i is really near the top of a developing cellular cloud feature in the WCR reflectivity imagery. The vertical structure of WCR reflectivity for each of the cloud water profiles in Fig. 1 was manually inspected. The three AC profiles in which the peak LWC was not within the upper half of the cloud water layer (i.e., Figs. 1a, 1g, and 1i) were all constructed from either direct descending or ascending flight tracks in the presence of some horizontal variability in the cloud structure. As a result, we are confident that the altitude of the peak LWC is within the upper half of the cloud and usually within tens of meters of cloud top, as would be expected in an adiabatic (i.e., well mixed) cloud profile.

The average thickness of the ice layer is 1180 m and varies from a minimum of 170 m to a maximum of 2240 m. With the exception of one case (Fig. 1i), the presence of ice is detected by the 2DC/2DP at or within tens of meters of cloud top and continues to cloud base, implying that most of the cloud layer is characterized by mixed-phase (i.e., coexisting liquid and ice water) conditions. On average, detectable mixed-phase cloud conditions begin 30 m below cloud top and were 310 m deep. Ice virga extends an average of 870 m beneath the cloud base but can be up to 1880 m deep. The bottom of the ice virga layer is as low (as warm) as about 2570 m ($-5.2°$C) but is on average located at 3990 m ($-9.7°$C). The peak IWC is typically found in the lower half of the combined mixed-phase cloud and ice virga layer. Visual inspection of the 2DC/2DP images within the mixed-phase cloud and virga below suggests that most ice particles were dendrites or irregularly shaped aggregates of dendrite, except in a narrow (e.g., 100–300 m) layer at cloud top where pristine crystals such as sector plates could be found, as is expected from laboratory experiments in this temperature range (e.g., Pruppacher and Klett 1997).

To summarize some relevant parameters for the 12 cases shown in Fig. 1, the upper, middle, and lower panels in the left column of Fig. 2 show the values of the maximum LWC versus the liquid cloud-base temperatures T_{LB}, the temperatures T_{LM} at the locations at which the maximum LWC values were observed, and the liquid cloud-top temperatures T_{LT}, respectively. The panels in the right column of Fig. 2 are similar to the left panels but are for IWC. It is evident that the maximum LWC values are approximately one order larger than the maximum IWC values. There is no obvious relationship between the maximum LWC and the temperature at which it occurs or the associated cloud-

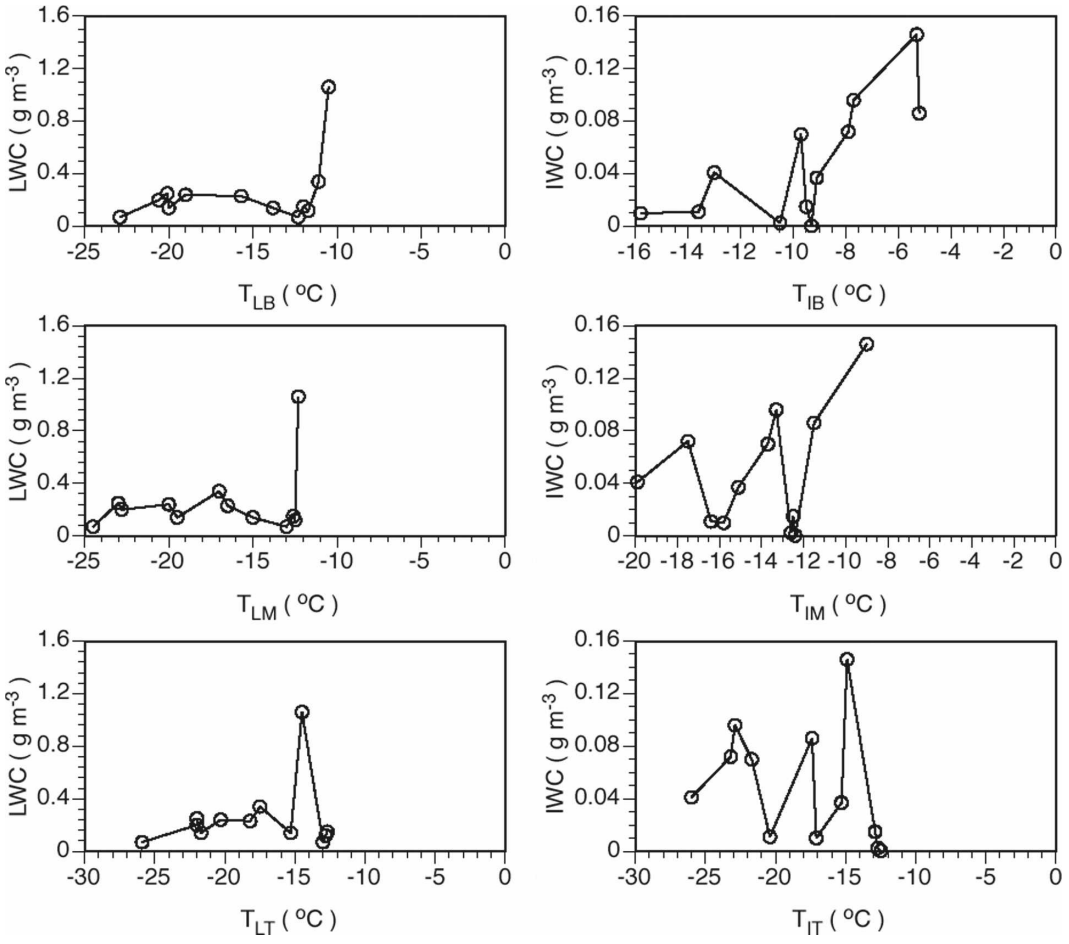

FIG. 2. (left) The maximum LWC vs the temperature of the liquid water cloud base T_{LB}, the temperature T_{LM} of the height at which the LWC maximum is observed, and the temperature of liquid water cloud top T_{LT}. (right) The maximum IWC vs the temperature of the ice water cloud base T_{IB}, the temperature T_{IM} of the height at which the IWC maximum is observed, and the temperature of ice water cloud top T_{IT}.

top or cloud-base temperatures, possibly because of the limited sample size. There is a weak tendency for larger maximum IWC to occur at warmer temperatures and to be associated with warmer ice water cloud base. The cloud-top temperatures for both liquid and ice clouds range from −12° to −26°C. However, the cloud-base temperatures for liquid clouds range from −10° to −22°C, whereas the counterparts for ice clouds range from −5° to −16°C. The evidence shows that all of these clouds are "cold" clouds.

Figure 3 is similar to Fig. 2, except that in Fig. 3 the maximum LWC and IWC values are plotted versus the cloud-base heights H_{LB}, the heights H_{LM} at the locations at which the maximum LWC and IWC values were observed, and the cloud-top heights H_{LT}. Again, there is no obvious relationship between the maximum LWC values and the heights that are observed. There is a tendency for larger maximum IWC to occur at lower heights and to be associated with lower ice cloud base and larger ice cloud depth.

4. Summary and discussion

Aircraft in situ measurements of the midlatitude midlevel mixed-phase AC clouds from October to November in 2001 over western Nebraska are analyzed. Ten flight missions in eight days provided 30 cloud water profiles associated with other specific observations. It is found that 20 out of the 30 cloud profiles are supercooled liquid–topped altocumulus clouds characterized by mixed-phase (i.e., coexistence of liquid water droplets and ice cloud particles) conditions beginning at or within tens of meters of cloud top and extending to the cloud base. The peak LWC occurs within the upper half of the liquid cloud layer and typically within tens of meters of cloud top. Ice virga is present well below

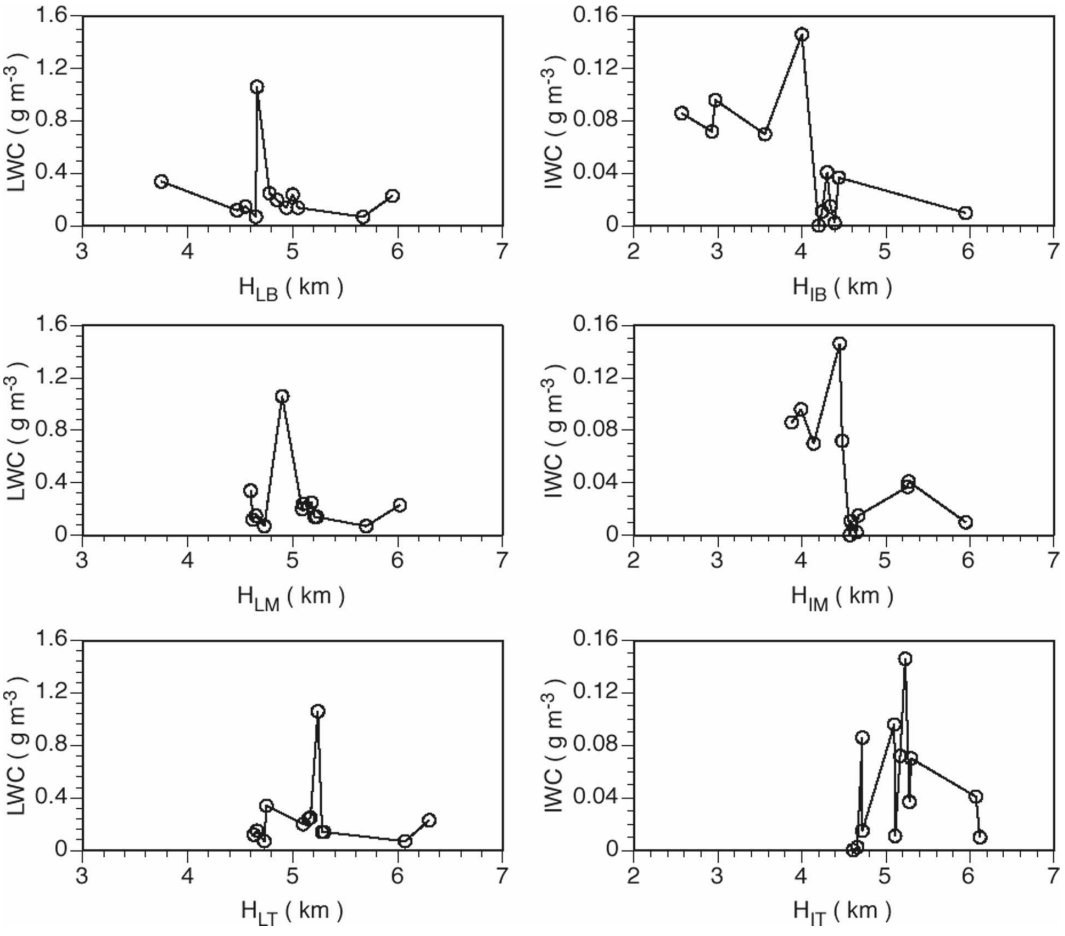

FIG. 3. (left) The maximum LWC vs the height of the liquid water cloud base H_{LB}, the height H_{LM} at which the LWC maximum is observed, and the temperature of liquid water cloud top H_{LT}. (right) The maximum IWC vs the height of the ice water cloud base H_{IB}, the height H_{IM} at which the IWC maximum is observed, and the height of ice water cloud top H_{IT}.

cloud base. The maximum IWC is typically found in the lower half of the combined mixed-phase cloud and ice virga layer. The estimation of IWC from particle size data requires an assumption regarding the particle mass–dimensional relation, resulting in potential error on the order of tens of percent. The overall results of this study are not sensitive to this potential source of error. This microphysical structure is very similar to those mixed-phase clouds that have been observed in the boundary layer over the Arctic region. We consider this specific cloud water profile as one of the common microphysical structures of midlevel mixed-phase AC clouds in the midlatitude region, and it should therefore be considered a paradigm for cloud radiative studies, satellite remote sensing algorithms, and cloud microphysical parameterizations. In the current study, we also noticed that another ⅓ of observed cloud profiles are ice dominated with little or no measurable supercooled liquid water content (i.e., glaciated). The study of these ice clouds will be documented elsewhere.

Another important motivation for this study is to provide guidance regarding the distribution of liquid and ice water substance in mixed-phase AC clouds for parameterization in climate models. In a number of highly advanced general circulation and cloud-resolving models (GCMs and CRMs, respectively) (e.g., Smith 1990; Bower et al. 1996; Rasch and Kristjansson 1998; Zhang et al. 2003; Khairoutdinov and Randall 2003), the partitioning of liquid and ice cloud water content is accomplished using simple parameterizations that are a function (e.g., linear or quadratic) only of temperature. In these parameterizations, the amount of ice (liquid) water substance decreases (increases) with increasing temperature. For example, in Khairoutdinov and Randall (2003) all cloud water substance is in ice form at temperatures below −20°C and the mass fraction of

liquid (ice) water increases (decreases) linearly to unity (zero) as the temperature approaches 0°C. Although seemingly intuitive, this simple microphysical parameterization cannot produce the correct vertical distribution of liquid and ice water content in midlevel mixed-phase AC clouds presented in this study. As reported in the literature (e.g., Sun and Shine 1995; McFarquhar and Cober 2004; Niu et al. 2008), this distribution of water mass is critical for the proper radiative transfer modeling in mixed-phase clouds and hence is potentially important for climatic-change studies.

The parameterization of ice and liquid water content in clouds within a GCM must take into account the frequency distribution of all cloud types (ice, liquid water, and mixed phase) as a function of temperature (e.g., Lin and Rossow 1996). Because we focus entirely on mixed-phase altocumulus clouds between 0° and −30°C, future studies should determine the relative frequency of these and other cloud types at midlatitudes.

It is important to point out that the observations herein apply strictly to nonprecipitating or weakly precipitating mixed-phase altocumulus clouds at midlatitudes. By comparison with past work, we can infer that our observations are also applicable to many nonprecipitating or weakly precipitating mixed-phase altocumulus and stratocumulus clouds at high latitudes (e.g., the Arctic). At midlatitudes, our mixed phase clouds typically occur under weak forcing (e.g., Fleishauer et al. 2002) and are therefore not the dominant cloud type under strongly forced conditions associated with precipitating storm systems (e.g., nimbostratus). Our results are not necessarily relevant for parameterizing clouds under these strongly forced conditions in CRMs. As such, there may be a way to use model mass flux in addition to temperature to parameterize mixed-phase clouds.

The in situ observations of 2 November are also unique because a long-lasting mixed-phase cloud (e.g., a cloud lifetime of 9–10 h is inferred from satellite infrared imagery) was sampled for several hours from sunrise to late morning as the cloud field dissipated. Of interest is that the sampled AC clouds appear to "deglaciate" (i.e., the IWC decreases dramatically as the LWC remains about the same) as the cloud system evolves from the early (Fig. 1j: 1323–1326 UTC) to the mature (Fig. 1k: 1434–1438 UTC) and then finally to the dissipation (Fig. 1l: 1618–1622 UTC) phase. The cloud radar and detailed microphysical structure of this deglaciating cloud system will be the subject of further study. Cloud deglaciation was noted in another midlevel mixed-phase cloud studied by Kankiewicz et al. (2000). More observations and further research are required to understand why ice production rapidly decelerated as the cloud field dissipated over Nebraska even while significant supercooled cloud water was still present. One potential hypothesis is that the available supply of ice nuclei for the cloud system was exhausted. However, ice nuclei measurements were not made during CLEX-9.

It is clear that more in situ observations of mixed-phase AC clouds, including ice nuclei measurements, are required to improve our understanding of their microphysical and radiative properties.

Acknowledgments. This research was supported by the DoD Center for Geosciences/Atmospheric Research at Colorado State University (CSU) under Cooperative Agreement DAAD19-02-2-0005 and W911NF-06-2-0015 with the Army Research Laboratory. Author P. Yang acknowledges support from the National Science Foundation (ATM-0239605) and the NASA Radiation Sciences Program (NNG04GL24G); V. E. Larson is grateful for financial support provided by ATM-0442605 from the National Science Foundation. We acknowledge the excellent support provided by the flight crew and scientific and technical staff of the University of Wyoming King Air Research Platform. We also thank the CSU forecasting team for their dedicated support during CLEX-9.

REFERENCESS

Baumgardner, D., 1983: An analysis and comparison of five water droplet measuring instruments. *J. Climate Appl. Meteor.,* **22,** 891–910.

Bower, K. N., S. J. Moss, D. W. Johnson, T. W. Choularton, J. Latham, P. R. A. Brown, A. M. Blyth, and J. Cardwell, 1996: A parametrization of the ice water content observed in frontal and convective clouds. *Quart. J. Roy. Meteor. Soc.,* **122,** 1815–1844.

Brown, P. R. A., and P. N. Francis, 1995: Improved measurement of the ice water content in cirrus using a total water probe. *J. Atmos. Oceanic Technol.,* **12,** 410–414.

Cerni, T., 1983: Determination of the size and concentration of cloud drops with an FSSP. *J. Climate Appl. Meteor.,* **22,** 1346–1355.

Cober, S. G., G. A. Isaac, and A. V. Korolev, 2001a: Assessing the Rosemount icing detector with in situ measurements. *J. Atmos. Oceanic Technol.,* **18,** 515–528.

——, ——, ——, and J. W. Strapp, 2001b: Assessing cloud-phase conditions. *J. Appl. Meteor.,* **40,** 1967–1983.

——, ——, and J. W. Strapp, 2001c: Characterizations of aircraft icing environments that include supercooled large drops. *J. Appl. Meteor.,* **40,** 1984–2002.

Fleishauer, R. P., V. E. Larson, and T. H. Vonder Haar, 2002: Observed microphysical structure of midlevel, mixed-phase clouds. *J. Atmos. Sci.,* **59,** 1779–1804.

Gregory, D., and D. Morris, 1996: The sensitivity of climate simulation to the specification of mixed-phase cloud. *Climate Dyn.,* **12,** 641–651.

Harrington, J. Y., T. Reisin, W. R. Cotton, and S. M. Kreidenweis,

1999: Cloud resolving simulations of Arctic stratus: Part II: Transition-season clouds. *Atmos. Res.,* **51,** 45–75.

Heymsfield, A., and J. Parrish, 1978: A computational technique for increasing the effective sampling volume of the PMS two-dimensional particle size spectrometer. *J. Appl. Meteor.,* **17,** 1566–1572.

——, L. M. Miloshevich, A. Slingo, K. Sassen, and D. O'C. Starr, 1991: An observational and theoretical study of highly supercooled altocumulus. *J. Atmos. Sci.,* **48,** 923–945.

——, S. Lewis, A. Bansemer, J. Iaquinta, L. M. Miloshevich, M. Kajikawa, C. Twohy, and M. R. Poellot, 2002: A general approach for deriving the properties of cirrus and stratiform ice cloud particles. *J. Atmos. Sci.,* **59,** 3–29.

Hobbs, P. V., and A. L. Rangno, 1985: Ice particle concentrations in clouds. *J. Atmos. Sci.,* **42,** 2523–2549.

——, and ——, 1998: Microstructures of low and middle-level clouds over the Beaufort Sea. *Quart. J. Roy. Meteor. Soc.,* **124,** 2035–2071.

——, ——, M. Shupe, and T. Uttal, 2001: Airborne studies of cloud structures over the Arctic Ocean and comparisons with retrievals from ship-based remote sensing measurements. *J. Geophys. Res.,* **106,** 15 029–15 044.

Hogan, R. J., P. N. Francis, H. Flentje, A. J. Illingworth, M. Quante, and J. Pelon, 2002: Characteristics of mixed-phase clouds Part I: Lidar, radar and aircraft observations from CLARE'98. *Quart. J. Roy. Meteor. Soc.,* **128,** 1–28.

Kankiewicz, J. A., R. P. Fleishauer, V. E. Larson, D. L. Reinke, J. M. Davis, T. H. Vonder Haar, and S. K. Cox, 2000: In-situ and satellite-based observations of mixed phase non-precipitating clouds and their environments. Preprints, *13th Int. Conf. on Clouds and Precipitation,* Reno, NV, International Commission on Clouds and Precipitation, 697–700.

Khairoutdinov, M. F., and D. A. Randall, 2003: Cloud resolving modeling of the ARM Summer 1997 IOP: Model formulation, results, uncertainties, and sensitivities. *J. Atmos. Sci.,* **60,** 607–625.

Korolev, A., G. A. Isaac, S. G. Cober, J. W. Strapp, and J. Hallett, 2003: Microphysical characterization of mixed-phase clouds. *Quart. J. Roy. Meteor. Soc.,* **129,** 39–65.

Larson, V. E., R. P. Fleishauer, J. A. Kankiewicz, D. L. Reinke, and T. H. Vonder Haar, 2001: The death of an altocumulus cloud. *Geophys. Res. Lett.,* **28,** 2609–2612.

Lawson, R. P., B. A. Baker, and C. G. Schmitt, 2001: An overview of microphysical properties of Arctic clouds observed in May and July 1998 during FIRE ACE. *J. Geophys. Res.,* **106,** 14 989–15 014.

Li, Z.-X., and H. Le Treut, 1992: Cloud-radiation feedbacks in a general circulation model and their dependence on cloud modeling assumptions. *Climate Dyn.,* **7,** 133–139.

Lin, B., and W. B. Rossow, 1996: Seasonal variation of liquid and ice water path in nonprecipitating clouds over oceans. *J. Climate,* **9,** 2890–2902.

McFarquhar, G. M., and S. G. Cober, 2004: Single-scattering properties of mixed-phase Arctic clouds at solar wavelengths: Impacts on radiative transfer. *J. Climate,* **17,** 3799–3813.

——, G. Zhang, M. R. Poellot, G. L. Kok, R. McCoy, T. Tooman, A. Fridlind, and A. J. Heymsfield, 2007: Ice properties of single-layer stratocumulus during the Mixed-Phase Arctic Cloud Experiment: 1. Observations. *J. Geophys. Res.*, **112,** D24201, doi:10.1029/2007JD008633.

Mitchell, D. L., R. Zhang, and R. Pitter, 1990: Mass-dimensional relationships for ice particles and the influence of riming on snowfall rate. *J. Appl. Meteor.,* **29,** 153–163.

Niu, J., L. D. Carey, P. Yang, and T. H. Vonder Haar, 2008: Optical properties of a vertically inhomogeneous mid-latitude mid-level mixed-phase altocumulus in the infrared region. *Atmos. Res.,* **88,** 234–242.

Pinto, J. O., 1998: Autumnal mixed-phase cloud boundary layers in the Arctic. *J. Atmos. Sci.,* **55,** 2016–2038.

——, J. A. Curry, and J. M. Intrieri, 2001: Cloud–aerosol interactions during autumn over Beaufort Sea. *J. Geophys. Res.,* **106,** 15 077–15 097.

Pruppacher, H. R., and J. D. Klett, 1997: *Microphysics of Clouds and Precipitation*. Kluwer Academic, 954 pp.

Rasch, P. J., and J. E. Kristjansson, 1998: A comparison of the CCM3 model climate using diagnosed and predicted condensate parameterizations. *J. Climate,* **11,** 1587–1614.

Rauber, R. M., and L. O. Grant, 1986: The characteristics and distribution of cloud water over the mountains of northern Colorado during wintertime storms. Part II: spatial distribution and microphysical characteristics. *J. Climate Appl. Meteor.,* **25,** 489–504.

Smith, R. N. B., 1990: A scheme for predicting layer clouds and their water content in a general circulation model. *Quart. J. Roy. Meteor. Soc.,* **116,** 435–460.

Sun, Z., and K. P. Shine, 1995: Parameterization of ice cloud radiative properties and its application to the potential climatic importance of mixed-phase clouds. *J. Climate,* **8,** 1874–1888.

Verlinde, J., and Coauthors, 2007: The Mixed-Phase Arctic Cloud Experiment. *Bull. Amer. Meteor. Soc.,* **88,** 205–221.

Wang, Z., K. Sassen, D. N. Whiteman, and B. B. Demoz, 2004: Studying altocumulus with ice virga using ground-based active and passive remote sensors. *J. Appl. Meteor.,* **43,** 449–460.

Yang, P., H. Wei, B. A. Baum, H. Huang, A. J. Heymsfield, Y. X. Hu, B. Gao, and D. D. Turner, 2003: The spectral signature of mixed-phase clouds composed of non-spherical ice crystals and spherical liquid droplets in the terrestrial window region. *J. Quant. Spectrosc. Radiat. Transfer,* **79-80,** 1171–1188.

Zhang, M., W. Lin, C. S. Bretherton, J. J. Hack, and P. J. Rasch, 2003: A modified formulation of fractional stratiform condensation rate in the NCAR Community Atmospheric Model (CAM2). *J. Geophys. Res.,* **108,** 4035, doi:10.1029/2002JD002523.

Zuidema, P., and Coauthors, 2005: An Arctic springtime mixed-phase cloudy boundary layer observed during SHEBA. *J. Atmos. Sci.,* **62,** 160–176.